

A Causal Convolutional Low-rank Representation Model for Imputation of Water Quality Data

Xin Liao

College of Computer and Information Science Southwest University Chongqing, China

lxchat26@gmail.com

Bing Yang

School of Environment and Ecology Chongqing University

Chongqing, China

cq_yangbing@163.com

Tan Dongli

Chongqing Eco-Environment Monitoring Center Chongqing, China

406865661@qq.com

Cai Yu*

Chongqing Eco-Environment Monitoring Center Chongqing, China

cyscut@foxmail.com

Abstract

The monitoring of water quality is a crucial part of environmental protection, and a large number of monitors are widely deployed to monitor water quality. Due to unavoidable factors such as data acquisition breakdowns, sensors and communication failures, water quality monitoring data suffers from missing values over time, resulting in High-Dimensional and Sparse (HDS) Water Quality Data (WQD). The simple and rough filling of the missing values leads to inaccurate results and affects the implementation of relevant measures. Therefore, this paper proposes a Causal convolutional Low-rank Representation (CLR) model for imputing missing WQD to improve the completeness of the WQD, which employs a two-fold idea: a) applying causal convolutional operation to consider the temporal dependence of the low-rank representation, thus incorporating temporal information to improve the imputation accuracy; and b) implementing a hyperparameters adaptation scheme to automatically adjust the best hyperparameters during model training, thereby reducing the tedious manual adjustment of hyper-parameters. Experimental studies on three real-world water quality datasets demonstrate that the proposed CLR model is superior to some of the existing state-of-the-art imputation models in terms of imputation accuracy and time cost, as well as indicating that the proposed model provides more reliable decision support for environmental monitoring.

Index Terms

Water quality data, High-dimensional and sparse, Data imputation, low-rank representation model, Causal convolutional, hyperparameters adaptation.

I. INTRODUCTION

Water quality monitoring plays a key role in environmental protection, public health and sustainable development. With the advancement of industrialization and intensification of human activities, water resource management becomes more and more important, and accurate Water Quality Data (WQD) provide a scientific basis for water resource management, pollution prevention and ecological protection [1]. By collecting WQD regularly, water quality trends are effectively identified and timely measures are taken to ensure water quality. However, the data recorded by widely deployed monitors are missing data due to equipment and transmission failures during data collection, and the High-Dimensional and Sparse (HDS) [2]–[8] WQD seriously affects data completeness, reliability, and hinders the accurate assessment of water quality monitoring. Therefore, how to precisely impute HDS data to provide subsequent analysis becomes a tricky task [9]–[11].

In recent years, researchers propose a variety of missing data imputation models to effectively impute missing values in data, such as K-Nearest Neighbors (KNN) imputation models, decision trees methods, Support Vector Machines (SVM) imputation, and deep learning approaches. Specifically, Murti *et al.* [12] adopt the KNN imputation to capture complex relationships in data and thus impute missing data, but it is difficult to effectively identify the true neighbors for high-dimensional data to provide accurate imputation. Rahman *et al.* [13] utilize decision trees to model complex relationships between features and capture nonlinear relationships to offer accurate imputation. However, this approach is easily suffer from the risk of overfitting. Brand *et al.* [14] apply SVM imputation to inscribe high-dimensional nonlinear relationships in the data and maintain robustness by regularizing the parameters, however it suffers from high computational complexity for large datasets. Samad *et al.* [15] propose an integrated learning-based imputation method that utilizes Deep Neural Networks (DNN) to replace linear regressors to improve the accuracy of imputing missing data. Unfortunately, deep learning approaches require considerable computational and time cost due to the large number of parameters computed [16]–[18].

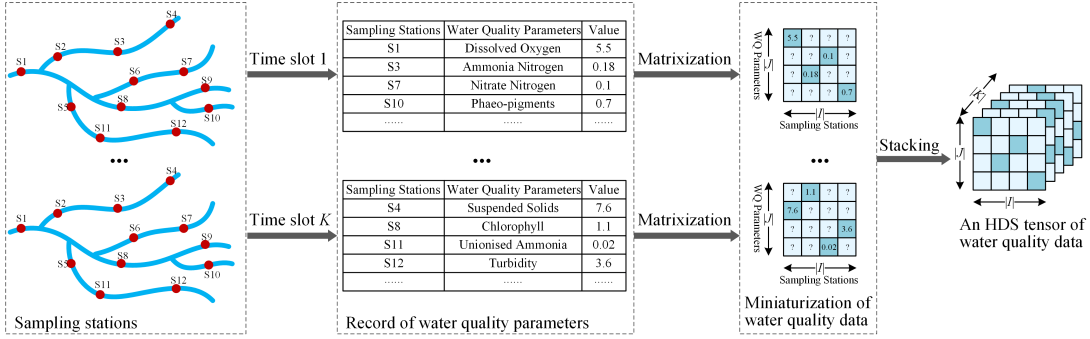


Fig. 1. An illustration of water quality data constructed as an HDS tensor.

TABLE I
THE DESCRIPTION FOR THE NOTATION

Notation	Description
I	A Set of sampling stations.
J	A set of water quality parameters.
K	A set of time slots.
\mathbf{X}	An HDS tensor constructed via the WQD.
$\tilde{\mathbf{X}}$	The low-rank approximation tensor of \mathbf{X} .
\mathbf{D}	rank-one tensors for $\tilde{\mathbf{X}}$.
$x_{ijk}, \tilde{x}_{ijk}, d_{ijk}$	A single element of $\mathbf{X}, \tilde{\mathbf{X}}$, and \mathbf{R} .
R	The number of rank-one tensors.
S, U, V	Three feature matrices correspond to I, J, K .
$\mathbf{s}_r, \mathbf{u}_r, \mathbf{v}_r$	The r -th column vectors of S, U , and V .
s_{ir}, u_{jr}, v_{kr}	An single element of S, U , and V .
\mathbf{W}	The weights of causal convolutional operator.
w_{cr}	An single weight of \mathbf{W} .
$\mathbf{a}, \mathbf{e}, \mathbf{o}$	Three linear bias vectors.
a_i, e_j, o_k	The single element of \mathbf{a}, \mathbf{e} , and \mathbf{o} .

Previous studies demonstrate that the Tensor Low-rank Representation (TLR) model can effectively deal with HDS data by modeling the features of the data via compact vector representations in the low-rank space to impute missing values in the HDS tensor [19]–[22]. On the other hand, the WQD can be represented as an HDS tensor presented in Fig. 1. Specifically, widely distributed sampling stations recorded monitoring data for each time slot, i.e., the monitoring values of the sampling stations for water quality parameters. By matrixizing the WQD for each time slot, a series of matrices arranged by time are obtained. Finally, an HDS tensor is constructed by stacking the above matrices, and its an elements denotes the monitoring value of the sampling station $i \in I$ for the water quality parameter $j \in J$ at the time slot $k \in K$. Therefore, we propose a Causal convolutional Low-rank Representation (CLR) model for imputing the WQD, which employs the causal convolutional operation and a Particle Swarm Optimization (PSO)-based [23]–[26] hyperparameters adaptation scheme to offer high imputation accuracy and low time cost [27]–[32]. The main contributions of this paper are listed as follows:

- A causal convolutional operator. It considers the temporal correlation of low-rank representations and efficiently models temporal features via causal characterization on the time, thereby providing accurate imputation accuracy.
- A PSO-based hyperparameters adaptation scheme. It avoids the tedious hyperparameters tuning process and adaptively adjusts the best hyperparameters during model training to reduce the model’s time overhead.
- An empirical study on three datasets. It demonstrates that the proposed CLR model outperforms several state-of-the-art imputation models in terms of imputation accuracy and time cost.

The remaining Sections are organized as follows: Section II presents the background, Section III introduces the proposed CLR model, Section IV and V provide experimental comparisons and conclusions, respectively.

II. BACKGROUND

A. Notation system

The notations employed in this paper are summarized in Table I. The tensor is denoted in uppercase bold, the matrix is denoted in uppercase, the vector is denoted in lowercase bold italic, and the scalar is denoted in lowercase italic.

B. Problem formulation

As presented in Fig. 1, the WQD can be represented by an HDS tensor, which is defined as:

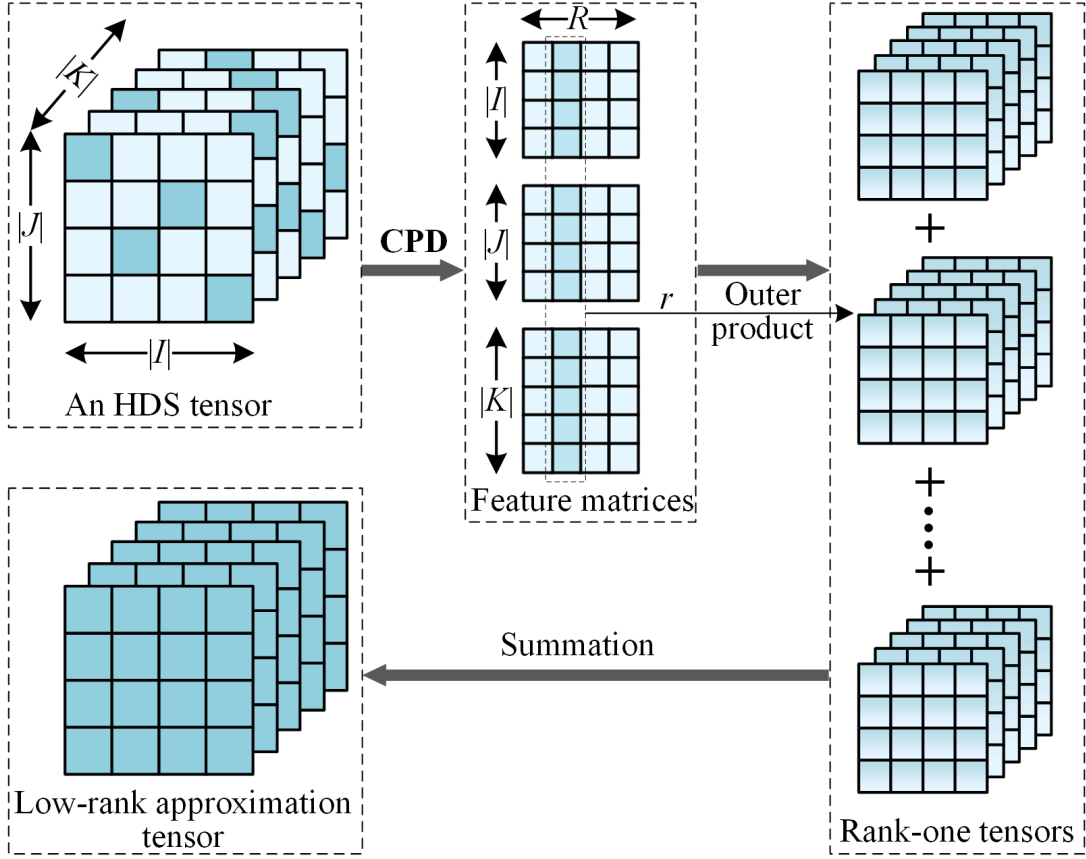


Fig. 2. An illustrative example of a tensor low-rank representation.

Definition 1. (HDS tensor). For a given tensor $\mathbf{X} \in \mathbb{R}^{|I| \times |J| \times |K|}$, let Ω and Υ denote the observed and unobserved element sets in the tensor, respectively. If $|\Upsilon| \gg |\Omega|$, the tensor \mathbf{X} is an HDS tensor, where a element x_{ijk} denotes a quantized value determined by the subscript (i, j, k) .

Following the CPD principle [33]–[36], the HDS tensor \mathbf{X} is decomposed into three low-rank feature matrices $\mathbf{S} \in \mathbb{R}^{|I| \times R}$, $\mathbf{U} \in \mathbb{R}^{|J| \times R}$, and $\mathbf{V} \in \mathbb{R}^{|K| \times R}$ to represent the sampling station features, water quality parameter features, and temporal features, respectively. R denotes the feature dimension also the number of rank-one tensors, i.e., the low-rank approximation tensor $\tilde{\mathbf{X}}$ is constructed by R rank-one tensors [37]–[40] as:

$$\tilde{\mathbf{X}} = \sum_{r=1}^R \mathbf{D}_r, \quad (1)$$

where the rank-one tensor \mathbf{D}_r is obtained by the outer product for the r -th column vectors of the three feature matrices, i.e. $\mathbf{D}_r = \mathbf{s}_r \circ \mathbf{u}_r \circ \mathbf{v}_r$. Therefore, the low-rank approximation tensor $\tilde{\mathbf{X}}$ is formulated as:

$$\tilde{\mathbf{X}} = \sum_{r=1}^R \mathbf{s}_r \circ \mathbf{u}_r \circ \mathbf{v}_r. \quad (2)$$

With a finer-grained representation, a single element \tilde{x}_{ijk} in $\tilde{\mathbf{X}}$ is obtained as:

$$\tilde{x}_{ijk} = \sum_{r=1}^R d_{ijk}^{(r)} = \sum_{r=1}^R s_{ir} u_{jr} v_{kr}. \quad (3)$$

With (1)–(3), an HDS tensor is low-rank represented by three feature matrices as illustrated in Fig. 2.

As indicated by previous studies [41]–[45], the low-rank representation models incorporating linear bias vectors are effective in suppressing fluctuations during model training process for the HDS data. Therefore, the element \tilde{x}_{ijk} is reformulated as:

$$\tilde{x}_{ijk} = \sum_{r=1}^R s_{ir} u_{jr} v_{kr} + a_i + e_j + o_k, \quad (4)$$

where a_i , e_j , and o_k are the elements of $\mathbf{a} \in \mathbb{R}^{|I|}$, $\mathbf{e} \in \mathbb{R}^{|J|}$, and $\mathbf{o} \in \mathbb{R}^{|K|}$ with subscripts i, j, k , respectively. To achieve the desired feature matrices and bias vectors, an objective function employing Euclidean distances [46]–[51] is commonly constructed to evaluate the difference between the original tensor and the approximated tensor. On the other hand, evaluating the gap for above two tensors on the observed element set Ω can effectively deal with data imbalance in the HDS tensor. Therefore, the objective function ε is constructed as:

$$\varepsilon = \frac{1}{2} \sum_{x_{ijk} \in \Omega} \left(x_{ijk} - \sum_{r=1}^R s_{ir} u_{jr} v_{kr} - a_i - e_j - o_k \right)^2. \quad (5)$$

To avoid overfitting of the model training, the L_2 regularization term is incorporated into the objective function as:

$$\begin{aligned} \varepsilon = & \frac{1}{2} \sum_{x_{ijk} \in \Omega} \left(x_{ijk} - \sum_{r=1}^R s_{ir} u_{jr} v_{kr} - a_i - e_j - o_k \right)^2 \\ & + \frac{\lambda}{2} \sum_{x_{ijk} \in \Omega} \left(\sum_{r=1}^R s_{ir}^2 + u_{jr}^2 + v_{kr}^2 + a_i^2 + e_j^2 + o_k^2 \right), \end{aligned} \quad (6)$$

where λ denote the regularization constants.

III. THE CLR MODEL

A. Objective function

As previously discussed, the WQD is an HDS tensor that contains time-varying information [52]–[58], i.e., the data in the k -th time slot influences the data in the $(k+1)$ -th time slot. Therefore, it is reasonable to implement the fusion of temporal information [59]–[61] on the current data by adopting the causal convolutional operator. Specifically, we employ local temporal information incorporation for the k -th time feature vector in the low-rank representation space as shown in Fig. 3. For the r -th column of the time feature vector, it is formulated as:

$$\bar{\mathbf{v}}_r = \mathbf{v}_r * \mathbf{w}_r, \quad (7)$$

where $*$ denotes the convolutional operator and $\mathbf{w}_r \in \mathbb{R}^C$ denotes the weight vector in the r -th channel. For an element \bar{v}_{kr} in the feature vector, it is fine-grained formulated as:

$$\bar{v}_{kr} = \sum_{c=1}^C v_{(k-c+1)r} w_{cr}. \quad (8)$$

Note that we employ zero padding to keep the length of the transformed vector constant. In addition, a sigmoid activation function is employed to capture nonlinear features, namely:

$$\tilde{v}_{kr} = \phi(\bar{v}_{kr}), \quad (9)$$

where ϕ denotes the Sigmoid activation function. By implementing the nonlinear mapping to the approximation, the \tilde{x}_{ijk} is reconstructed as:

$$\tilde{x}_{ijk} = \phi \left(\sum_{r=1}^R s_{ir} u_{jr} \tilde{v}_{kr} + a_i + e_j + o_k \right). \quad (10)$$

Hence, the objective function of the proposed CLR model is constructed as:

$$\begin{aligned} \varepsilon = & \frac{1}{2} \sum_{x_{ijk} \in \Omega} \left(x_{ijk} - \phi \left(\sum_{r=1}^R s_{ir} u_{jr} \tilde{v}_{kr} + a_i + e_j + o_k \right) \right)^2 \\ & + \frac{\lambda}{2} \sum_{x_{ijk} \in \Omega} \left(\sum_{r=1}^R s_{ir}^2 + u_{jr}^2 + v_{kr}^2 + \sum_{c=1}^C w_{cr}^2 + a_i^2 + e_j^2 + o_k^2 \right) \end{aligned} \quad (11)$$

B. Parameters learning

In order to learn the required model parameters, we use the standard Stochastic Gradient Descent (SGD) [62], [63] algorithm to update the feature matrices, bias vectors, and convolution kernel weights due to its simplicity, efficiency, and applicability to large-scale datasets [64]–[70]. Its learning rule is as:

$$\theta^{t+1} = \theta^t - \eta \nabla_{\theta} (\theta^t), \quad (12)$$

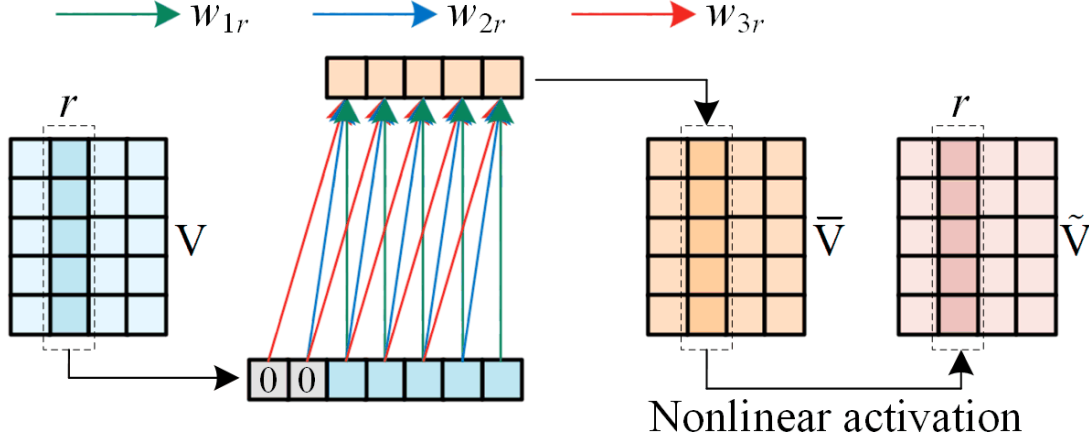


Fig. 3. An illustration of the causal convolutional transform for the time feature matrix with a 3×1 convolution kernel size.

where θ denotes the model parameters, t denotes the iteration round, and η denotes the learning rate. Therefore, the stochastic gradients of the model parameters (The derivations of s_{ir} and a_i apply to u_{jr} , e_j and o_k , respectively.) are given as:

$$\begin{cases} \frac{\partial \varepsilon_{ijk}}{\partial s_{ir}} = \varphi_{ijk} (u_{jr} \tilde{v}_{kr}) + \lambda s_{ir} \\ \frac{\partial \varepsilon_{ijk}}{\partial v_{kr}} = \varphi_{ijk} (s_{ir} u_{jr} \tilde{v}_{kr} (1 - \tilde{v}_{kr}) w_{1r}) + \lambda v_{kr} \\ \frac{\partial \varepsilon_{ijk}}{\partial w_{cr}} = \varphi_{ijk} (s_{ir} u_{jr} \tilde{v}_{kr} (1 - \tilde{v}_{kr}) v_{(k-c+1)r}) + \lambda w_{cr} \\ \frac{\partial \varepsilon_{ijk}}{\partial a_i} = \varphi_{ijk} + \lambda a_i \end{cases} \quad (13)$$

where $\varphi_{ijk} = -(x_{ijk} - \tilde{x}_{ijk}) \tilde{x}_{ijk} (1 - \tilde{x}_{ijk})$. With (12), their update rules are as:

$$\begin{cases} s_{ir}^{t+1} = s_{ir}^t - \eta (\varphi_{ijk} (u_{jr} \tilde{v}_{kr}) + \lambda s_{ir}^t) \\ v_{kr}^{t+1} = v_{kr}^t - \eta (\varphi_{ijk} (s_{ir} u_{jr} \tilde{v}_{kr} (1 - \tilde{v}_{kr}) w_{1r}) + \lambda v_{kr}^t) \\ w_{cr}^{t+1} = w_{cr}^t - \eta (\varphi_{ijk} (s_{ir} u_{jr} \tilde{v}_{kr} (1 - \tilde{v}_{kr}) v_{(k-c+1)r}) + \lambda w_{cr}^t) \\ a_i^{t+1} = a_i^t - \eta (\varphi_{ijk} + \lambda a_i^t) \end{cases} \quad (14)$$

C. The PSO-based Hyperparameters Adaptation

The learning of model parameters relies on two hyperparameters η and λ . We adopt a PSO-based hyperparameters adaptation scheme to reduce the large time overhead suffered by manually tuning. Specifically, P particles are initialized, where the velocity and position of the p -th particle are defined by two vectors, $\mathbf{m}_{(p)} = (\eta_{(p)}, \lambda_{(p)})$ and $\mathbf{n}_{(p)} = (n_{\eta_{(p)}}, n_{\lambda_{(p)}})$, $p = \{1, 2, \dots, P\}$. Following the PSO principle, p -th particle is updated as:

$$\begin{cases} \mathbf{n}_{(p)}^{t+1} = \omega \mathbf{n}_{(p)}^t + c_1 r_1 (\mathbf{pb}_{(p)}^t - \mathbf{m}_{(p)}^t) + c_2 r_2 (\mathbf{gb}^t - \mathbf{m}_{(p)}^t), \\ \mathbf{m}_{(p)}^{t+1} = \mathbf{m}_{(p)}^t + \mathbf{n}_{(p)}^{t+1}, \end{cases} \quad (15)$$

where ω denotes the inertia constant, c_1 and c_2 denote the factors, r_1 and r_2 denote the random values in the scale of $[0, 1]$, $\mathbf{pb}_{(p)}$ and \mathbf{gb} denote individual and global optimums, respectively. To evaluate the performance gain of each particle, we adopt the fitness function as:

$$F_{(p)}^{t+1} = \frac{Q(\mathbf{m}_{(p)}^{t+1}) - Q(\mathbf{m}_{(p-1)}^{t+1})}{Q(\mathbf{m}_{(P)}^{t+1}) - Q(\mathbf{m}_{(P)}^t)}, \quad (16)$$

where $Q(\mathbf{m}_{(0)}^{t+1}) = Q(\mathbf{m}_{(P)}^t)$ and Q is defined as:

$$Q(\mathbf{m}_{(p)}) = \sqrt{\sum_{x_{ijk} \in \Lambda} (x_{ijk} - \tilde{x}_{ijk(p)})^2 / |\Lambda|}, \quad (17)$$

where Λ denotes the validation set from the unobserved element set. Therefore, the update rules of model parameters with the hyperparameters adaptation are given as (Taking s_{ir} for example):

$$s_{ir(p)}^{t+1} = s_{ir(p)}^t - \eta_{(p)} (\varphi_{ijk} (u_{jr} \tilde{v}_{kr}) + \lambda_{(p)} s_{ir(p)}^t). \quad (18)$$

Algorithm 1: CLR model

```

Initialize  $\Omega, I, J, K, R, \mathbf{m}, \mathbf{n}, P, T$  ;
Initialize  $S, U, V, \mathbf{a}, \mathbf{e}, \mathbf{o}, W$  with positive values;
while  $t \leq T$  and not converge do
  foreach  $p = 1$  to  $P$  do
    Update model parameters  $\theta$  ;
  Compute  $Q(\mathbf{m}_{(p)}^t)$ ;
  foreach  $p = 1$  to  $P$  do
    Compute  $F(\mathbf{m}_{(p)}^t)$ ;
    update  $\mathbf{pb}_{(p)}^t$  and  $\mathbf{gb}^t$ ;
   $t = t + 1$ ;

```

TABLE II
THE IMPUTATION ACCURACY FOR FIVE TESTED MODELS

Dataset		M1	M2	M3	M4	M5
D1	RMSE	0.0246	0.0256	0.0260	0.0273	0.0267
	MAE	0.0131	0.0162	0.0148	0.0162	0.0163
D2	RMSE	0.0257	0.0262	0.0266	0.0287	0.0270
	MAE	0.0152	0.0175	0.0161	0.0177	0.0176
D3	RMSE	0.0249	0.0258	0.0262	0.0277	0.0259
	MAE	0.0158	0.0176	0.0159	0.0175	0.0166

With (18), the proposed CLR algorithm implements the learning of model parameters and automatically updates of hyperparameters. The specific process of the model is presented in Algorithm 1.

IV. EXPERIMENTAL COMPARISONS

A. Datasets

In this paper, we evaluate the performance of the proposed model on three real-world water quality datasets. They are derived from 24 sampling stations of the Hong Kong Environmental Protection Department in Victoria Harbour for 24 water quality parameters over 903 time slots, where D1 contains 129406 surface observed WQD, D2 contains 121218 middle depth observed WQD, and D3 contains 129415 bottom observed WQD. Further, the datasets are divided into the training set (Γ), the validation set (Λ), and the test set (Φ) with 1:2:7. For all experiments, all tested models are run twenty times to provide unbiased average results.

B. Evaluation metrics

In order to fairly measure the performance of the models, the prevalent Root Mean Squared Error (RMSE) and Mean Absolute Error (MAE) [71]–[76] are adopted for evaluating the metrics as:

$$\begin{aligned}
 \text{RMSE} &= \sqrt{\sum_{x_{ijk} \in \Phi} (x_{ijk} - \tilde{x}_{ijk})^2 / |\Phi|}; \\
 \text{MAE} &= \sum_{x_{ijk} \in \Phi} |x_{ijk} - \tilde{x}_{ijk}|_{\text{abs}} / |\Phi|,
 \end{aligned} \tag{19}$$

where $|\cdot|_{\text{abs}}$ denotes the absolute value. Note smaller RMSE and MAE indicate better imputation accuracy.

C. Comparison Results

We compare the results of the proposed CLR model with four state-of-the-art imputation models on three datasets in terms of imputation accuracy and time cost. The tested models are: a) M1: The proposed CLR model; b) M2 [7]: A biased low-rank representation model for imputation that learns model parameters via the nonnegative update algorithm; c) M3 [77]: A robust imputation model employing the Cauchy loss function; d) M4 [78]: A multilinear imputation model with integrated reconfiguration optimization algorithm; e) M5 [79]: A multidimensional imputation model employing the alternating least squares algorithm.

TABLE III
THE TIME COST FOR FIVE TESTED MODELS (SECS.)

Dataset		M1	M2	M3	M4	M5
D1	Time-R	1.457	3.268	5.716	20.03	4.984
	Time-M	1.311	4.297	3.576	20.14	3.971
D2	Time-R	1.922	4.518	4.823	15.71	7.324
	Time-M	1.820	6.248	3.862	16.42	7.146
D3	Time-R	1.796	2.465	3.146	16.65	11.06
	Time-M	1.672	3.162	4.597	17.51	11.15

The rank of all models are set to 10 and the iteration rounds are set to 1000. Note that the tested models are terminated if the error in two consecutive iteration rounds is less than 10^{-5} . Tables II and III present the statistical results, and it can be observed that:

- *The CLR model presents higher imputation accuracy compared with its peers.* As shown in Table II, the RMSE and MAE on D2 of M1 are 0.0257 and 0.0152, respectively. It improves by 1.90% and 13.14%, 3.38% and 5.59%, 10.45% and 14.12%, 4.48% and 13.63% compared to 0.0262 and 0.0175, 0.0266 and 0.0161, 0.0287 and 0.0177, 0.0270 and 0.0176 of M2-M5, respectively. Similar performance comparisons are also observed on other datasets.
- *The CLR model exhibits less time cost compared with its peers.* For the statistical results in Table III, M1 costs 1.922 seconds in RMSE and 1.820 seconds in MAE on D2. Compared to M2's 4.518 and 6.248, M3's 4.823 and 3.862, M4's 15.71 and 16.42, M5's 7.324 and 7.146, M1's time cost in RMSE and MAE are only their 42.54% and 29.12%, 39.85% and 47.12%, 12.23% and 11.08%, 26.24% and 25.46%, respectively. On the other two datasets, the time cost of M1 are similarly less than that of the comparison models.

Based on the above analysis, the proposed CLR model achieves higher imputation accuracy and less time cost against to the other imputation models.

V. CONCLUSIONS

To achieve precise imputation of missing data, this paper proposes a low-rank representation model with higher imputation accuracy and less time cost. Specifically, it employs a causal convolution operator to model temporal features and fuse temporal information. In addition, it achieves efficient model training via an adaptation scheme. Model performance evaluation on three water quality datasets indicated that the proposed model outperforms existing imputation models for imputing the missing data. For future work, we plan to explore the low-rank representation of spatial information [80]–[83].

REFERENCES

- [1] D. Zeng, L. Gu, L. Lian, H. Yao, and J. Hu, "On cost-efficient sensor placement for contaminant detection in water distribution systems," *IEEE Trans. Ind. Informat.*, vol. 12, no. 6, pp. 2177–2185, 2016.
- [2] H. Wu, Y. Qiao, and X. Luo, "A fine-grained regularization scheme for nonnegative latent factorization of high-dimensional and incomplete tensors," *IEEE Trans. Serv. Comput.*, vol. 17, no. 6, pp. 3006–3021, 2024.
- [3] H. Wu and J. Mi, "A cauchy loss-incorporated nonnegative latent factorization of tensors model for spatiotemporal traffic data recovery," *Neurocomputing*, p. 129575, 2025.
- [4] P. Tang, T. Ruan, H. Wu, and X. Luo, "Temporal pattern-aware qos prediction by biased non-negative tucker factorization of tensors," *Neurocomputing*, vol. 582, p. 127447, 2024.
- [5] H. Wu, X. Luo, and M. Zhou, "Advancing non-negative latent factorization of tensors with diversified regularization schemes," *IEEE Transactions on Services Computing*, vol. 15, no. 3, pp. 1334–1344, 2020.
- [6] H. Wu, X. Luo, M. Zhou, M. J. Rawa, K. Sedraoui, and A. Albeshri, "A pid-incorporated latent factorization of tensors approach to dynamically weighted directed network analysis," *IEEE/CAA Journal of Automatica Sinica*, vol. 9, no. 3, pp. 533–546, 2021.
- [7] X. Luo, H. Wu, H. Yuan, and M. Zhou, "Temporal pattern-aware qos prediction via biased non-negative latent factorization of tensors," *IEEE transactions on cybernetics*, vol. 50, no. 5, pp. 1798–1809, 2019.
- [8] X. Luo, H. Wu, Z. Wang, J. Wang, and D. Meng, "A novel approach to large-scale dynamically weighted directed network representation," *IEEE Transactions on Pattern Analysis and Machine Intelligence*, vol. 44, no. 12, pp. 9756–9773, 2021.
- [9] X. Liao, K. Hoang, and X. Luo, "Local search-based anytime algorithms for continuous distributed constraint optimization problems," *IEEE/CAA Journal of Automatica Sinica*, vol. 12, no. 1, pp. 288–290, 2025.
- [10] X. Luo, H. Wu, and Z. Li, "Neulfit: A novel approach to nonlinear canonical polyadic decomposition on high-dimensional incomplete tensors," *IEEE Transactions on Knowledge and Data Engineering*, 2022.
- [11] H. Wu and X. Luo, "Instance-frequency-weighted regularized, nonnegative and adaptive latent factorization of tensors for dynamic qos analysis," in *2021 IEEE International Conference on Web Services (ICWS)*. IEEE, 2021, pp. 560–568.
- [12] D. M. P. Murti, U. Pujianto, A. P. Wibawa, and M. I. Akbar, "K-nearest neighbor (k-nn) based missing data imputation," in *5th International Conference on Science in Information Technology*, 2019, pp. 83–88.
- [13] M. G. Rahman and M. Z. Islam, "Missing value imputation using decision trees and decision forests by splitting and merging records: Two novel techniques," *Knowl.-Based Syst.*, vol. 53, pp. 51–65, 2013.
- [14] L. Brand, L. Z. Baker, and H. Wang, "A multi-instance support vector machine with incomplete data for clinical outcome prediction of covid-19," in *proceedings of the 12th ACM conference on bioinformatics, computational biology, and health informatics*, 2021, pp. 1–6.
- [15] M. D. Samad, S. Abrar, and N. Diawara, "Missing value estimation using clustering and deep learning within multiple imputation framework," *Knowl.-Based Syst.*, vol. 249, p. 108968, 2022.
- [16] X. Luo, M. Chen, H. Wu, Z. Liu, H. Yuan, and M. Zhou, "Adjusting learning depth in nonnegative latent factorization of tensors for accurately modeling temporal patterns in dynamic qos data," *IEEE Transactions on Automation Science and Engineering*, vol. 18, no. 4, pp. 2142–2155, 2021.

- [17] Q. Wang and H. Wu, "Dynamically weighted directed network link prediction using tensor ring decomposition," in *2024 27th International Conference on Computer Supported Cooperative Work in Design (CSCWD)*. IEEE, 2024, pp. 2864–2869.
- [18] P. Jiao, X. Guo, X. Jing, D. He, H. Wu, S. Pan, M. Gong, and W. Wang, "Temporal network embedding for link prediction via vae joint attention mechanism," *IEEE Transactions on Neural Networks and Learning Systems*, vol. 33, no. 12, pp. 7400–7413, 2021.
- [19] M. Shi, X. Liao, and Y. Chen, "A dual-population search differential evolution algorithm for functional distributed constraint optimization problems," *Annals of Mathematics and Artificial Intelligence*, vol. 90, no. 10, pp. 1055–1078, 2022.
- [20] H. Wu, X. Luo, and M. Zhou, "Neural latent factorization of tensors for dynamically weighted directed networks analysis," in *2021 IEEE International Conference on Systems, Man, and Cybernetics (SMC)*. IEEE, 2021, pp. 3061–3066.
- [21] X. Xu, M. Lin, X. Luo, and Z. Xu, "Hr-st-lr: a hessian regularization spatio-temporal low rank algorithm for traffic data imputation," *IEEE Transactions on Intelligent Transportation Systems*, vol. 24, no. 10, pp. 11001–11017, 2023.
- [22] H. Wu, Y. Xia, and X. Luo, "Proportional-integral-derivative-incorporated latent factorization of tensors for large-scale dynamic network analysis," in *2021 China Automation Congress (CAC)*. IEEE, 2021, pp. 2980–2984.
- [23] M. Shi, X. Liao, and Y. Chen, "A particle swarm with local decision algorithm for functional distributed constraint optimization problems," *International journal of pattern recognition and artificial intelligence*, vol. 36, no. 12, p. 2259025, 2022.
- [24] X. Luo, J. Chen, Y. Yuan, and Z. Wang, "Pseudo gradient-adjusted particle swarm optimization for accurate adaptive latent factor analysis," *IEEE Transactions on Systems, Man, and Cybernetics: Systems*, 2024.
- [25] X. Luo, Y. Yuan, S. Chen, N. Zeng, and Z. Wang, "Position-transitional particle swarm optimization-incorporated latent factor analysis," *IEEE Transactions on Knowledge and Data Engineering*, vol. 34, no. 8, pp. 3958–3970, 2020.
- [26] L. Hu, Y. Yang, Z. Tang, Y. He, and X. Luo, "Fcan-mopso: an improved fuzzy-based graph clustering algorithm for complex networks with multiobjective particle swarm optimization," *IEEE Transactions on Fuzzy Systems*, vol. 31, no. 10, pp. 3470–3484, 2023.
- [27] H. Fang, Q. Wang, Q. Hu, and H. Wu, "Modularity maximization-incorporated nonnegative tensor rescal decomposition for dynamic community detection," in *2024 IEEE International Conference on Systems, Man, and Cybernetics (SMC)*. IEEE, 2024, pp. 1871–1876.
- [28] G. Liu and H. Wu, "Hp-csf: An gpu optimization method for cp decomposition of incomplete tensors," in *IFIP International Conference on Network and Parallel Computing*. Springer, 2024, pp. 77–90.
- [29] H. Wu, X. Wu, and X. Luo, *Dynamic Network Representation Based on Latent Factorization of Tensors*. Springer, 2023.
- [30] X. Liao and K. D. Hoang, "A population-based search approach to solve continuous distributed constraint optimization problems," *Applied Sciences*, vol. 14, no. 3, p. 1290, 2024.
- [31] C. Ren and Y. Xu, "A fully data-driven method based on generative adversarial networks for power system dynamic security assessment with missing data," *IEEE Transactions on Power Systems*, vol. 34, no. 6, pp. 5044–5052, 2019.
- [32] J.-P. Onnela, J. Saramäki, J. Hyvönen, G. Szabó, M. A. De Menezes, K. Kaski, A.-L. Barabási, and J. Kertész, "Analysis of a large-scale weighted network of one-to-one human communication," *New journal of physics*, vol. 9, no. 6, p. 179, 2007.
- [33] Y.-L. Li, Z.-H. Zhan, Y.-J. Gong, W.-N. Chen, J. Zhang, and Y. Li, "Differential evolution with an evolution path: A deep evolutionary algorithm," *IEEE transactions on cybernetics*, vol. 45, no. 9, pp. 1798–1810, 2014.
- [34] Q. Zhang, L. T. Yang, Z. Chen, and P. Li, "An improved deep computation model based on canonical polyadic decomposition," *IEEE Transactions on Systems, Man, and Cybernetics: Systems*, vol. 48, no. 10, pp. 1657–1666, 2017.
- [35] I. Dokmanic, R. Parhizkar, J. Ranieri, and M. Vetterli, "Euclidean distance matrices: essential theory, algorithms, and applications," *IEEE Signal Processing Magazine*, vol. 32, no. 6, pp. 12–30, 2015.
- [36] P. Shah, U. K. Khankhoje, and M. Moghaddam, "Inverse scattering using a joint $l_1 - l_2$ norm-based regularization," *IEEE Transactions on Antennas and Propagation*, vol. 64, no. 4, pp. 1373–1384, 2016.
- [37] Q. Wang, X. Liao, and H. Wu, "Biased block term tensor decomposition for temporal pattern-aware qos prediction," *International Journal of Pattern Recognition and Artificial Intelligence*, 2025.
- [38] X. Liao, Q. Hu, and P. Tang, "An adaptive temporal-dependent tensor low-rank representation model for dynamic communication network embedding," in *2024 International Conference on Networking, Sensing and Control (ICNSC)*. IEEE, 2024, pp. 1–6.
- [39] Z. Zhang, F. Zhuang, H. Zhu, Z. Shi, H. Xiong, and Q. He, "Relational graph neural network with hierarchical attention for knowledge graph completion," in *Proceedings of the AAAI conference on artificial intelligence*, vol. 34, no. 05, 2020, pp. 9612–9619.
- [40] C. Lee, J. Yoon, and M. Van Der Schaar, "Dynamic-deephit: A deep learning approach for dynamic survival analysis with competing risks based on longitudinal data," *IEEE Transactions on Biomedical Engineering*, vol. 67, no. 1, pp. 122–133, 2019.
- [41] Y. Song, M. Li, Z. Zhu, G. Yang, and X. Luo, "Nonnegative latent factor analysis-incorporated and feature-weighted fuzzy double c -means clustering for incomplete data," *IEEE Transactions on Fuzzy Systems*, vol. 30, no. 10, pp. 4165–4176, 2022.
- [42] D. Wu, Z. Li, Z. Yu, Y. He, and X. Luo, "Robust low-rank latent feature analysis for spatiotemporal signal recovery," *IEEE Transactions on Neural Networks and Learning Systems*, 2023.
- [43] F. Bi, X. Luo, B. Shen, H. Dong, and Z. Wang, "Proximal alternating-direction-method-of-multipliers-incorporated nonnegative latent factor analysis," *IEEE/CAA Journal of Automatica Sinica*, vol. 10, no. 6, pp. 1388–1406, 2023.
- [44] S. Deng, Q. Hu, D. Wu, and Y. He, "Btc-ksm: A blockchain-assisted threshold cryptography for key security management in power iot data sharing," *Computers and Electrical Engineering*, vol. 108, p. 108666, 2023.
- [45] Y. Yuan, X. Luo, M. Shang, and Z. Wang, "A kalman-filter-incorporated latent factor analysis model for temporally dynamic sparse data," *IEEE Transactions on Cybernetics*, 2022.
- [46] D. Wu, Q. He, X. Luo, M. Shang, Y. He, and G. Wang, "A posterior-neighborhood-regularized latent factor model for highly accurate web service qos prediction," *IEEE Transactions on Services Computing*, vol. 15, no. 2, pp. 793–805, 2019.
- [47] F. Ye, Z. Lin, C. Chen, Z. Zheng, and H. Huang, "Outlier-resilient web service qos prediction," in *Proceedings of the Web Conference 2021*, 2021, pp. 3099–3110.
- [48] S. Wang, Y. Ma, B. Cheng, F. Yang, and R. N. Chang, "Multi-dimensional qos prediction for service recommendations," *IEEE Transactions on Services Computing*, vol. 12, no. 1, pp. 47–57, 2016.
- [49] X. Su, M. Zhang, Y. Liang, Z. Cai, L. Guo, and Z. Ding, "A tensor-based approach for the qos evaluation in service-oriented environments," *IEEE Transactions on Network and Service Management*, vol. 18, no. 3, pp. 3843–3857, 2021.
- [50] D. Wu, P. Zhang, Y. He, and X. Luo, "A double-space and double-norm ensemble latent factor model for highly accurate web service qos prediction," *IEEE Transactions on Services Computing*, vol. 16, no. 2, pp. 802–814, 2022.
- [51] D. Wu, X. Luo, Y. He, and M. Zhou, "A prediction-sampling-based multilayer-structured latent factor model for accurate representation to high-dimensional and sparse data," *IEEE Transactions on Neural Networks and Learning Systems*, vol. 35, no. 3, pp. 3845–3858, 2022.
- [52] J. Chen, R. Wang, D. Wu, and X. Luo, "A differential evolution-enhanced position-transitional approach to latent factor analysis," *IEEE Transactions on Emerging Topics in Computational Intelligence*, vol. 7, no. 2, pp. 389–401, 2022.
- [53] W. Qin, X. Luo, S. Li, and M. Zhou, "Parallel adaptive stochastic gradient descent algorithms for latent factor analysis of high-dimensional and incomplete industrial data," *IEEE Transactions on Automation Science and Engineering*, 2023.
- [54] D. Wu, P. Zhang, Y. He, and X. Luo, "Mmlf: Multi-metric latent feature analysis for high-dimensional and incomplete data," *IEEE Transactions on Services Computing*, 2023.
- [55] Y. Yuan, X. Luo, and M. Zhou, "Adaptive divergence-based non-negative latent factor analysis of high-dimensional and incomplete matrices from industrial applications," *IEEE Transactions on Emerging Topics in Computational Intelligence*, 2024.

- [56] W. Li, R. Wang, and X. Luo, "A generalized nesterov-accelerated second-order latent factor model for high-dimensional and incomplete data," *IEEE Transactions on Neural Networks and Learning Systems*, 2023.
- [57] Z. Liu, X. Luo, and M. Zhou, "Symmetry and graph bi-regularized non-negative matrix factorization for precise bi community detection," *IEEE Transactions on Automation Science and Engineering*, vol. 21, no. 2, pp. 1406–1420, 2023.
- [58] J. Li, X. Luo, Y. Yuan, and S. Gao, "A nonlinear pid-incorporated adaptive stochastic gradient descent algorithm for latent factor analysis," *IEEE Transactions on Automation Science and Engineering*, 2023.
- [59] L. Hu, S. Yang, X. Luo, and M. Zhou, "An algorithm of inductively identifying clusters from attributed graphs," *IEEE Transactions on Big Data*, vol. 8, no. 2, pp. 523–534, 2020.
- [60] X. Luo, Y. Zhong, Z. Wang, and M. Li, "An alternating-direction-method of multipliers-incorporated approach to symmetric non-negative latent factor analysis," *IEEE Transactions on Neural Networks and Learning Systems*, vol. 34, no. 8, pp. 4826–4840, 2021.
- [61] W. Li, X. Luo, H. Yuan, and M. Zhou, "A momentum-accelerated hessian-vector-based latent factor analysis model," *IEEE Transactions on Services Computing*, vol. 16, no. 2, pp. 830–844, 2022.
- [62] J. Chen, Y. Yuan, and X. Luo, "Sdgnn: Symmetry-preserving dual-stream graph neural networks," *IEEE/CAA Journal of Automatica Sinica*, vol. 11, no. 7, pp. 1717–1719, 2024.
- [63] J. Wang, W. Li, and X. Luo, "A distributed adaptive second-order latent factor analysis model," *IEEE/CAA Journal of Automatica Sinica*, 2024.
- [64] M. Chen, R. Wang, Y. Qiao, and X. Luo, "Ageneralized nesterov's accelerated gradient-incorporated non-negative latent-factorization-of-tensors model for efficient representation to dynamic qos data," *IEEE Transactions on Emerging Topics in Computational Intelligence*, 2024.
- [65] X. Luo, Y. Zhou, Z. Liu, L. Hu, and M. Zhou, "Generalized nesterov's acceleration-incorporated, non-negative and adaptive latent factor analysis," *IEEE Transactions on Services Computing*, vol. 15, no. 5, pp. 2809–2823, 2021.
- [66] X. Luo, Z. Liu, L. Jin, Y. Zhou, and M. Zhou, "Symmetric nonnegative matrix factorization-based community detection models and their convergence analysis," *IEEE Transactions on Neural Networks and Learning Systems*, vol. 33, no. 3, pp. 1203–1215, 2021.
- [67] X. Shi, Q. He, X. Luo, Y. Bai, and M. Shang, "Large-scale and scalable latent factor analysis via distributed alternative stochastic gradient descent for recommender systems," *IEEE Transactions on Big Data*, vol. 8, no. 2, pp. 420–431, 2020.
- [68] Y. Yuan, Q. He, X. Luo, and M. Shang, "A multilayered-and-randomized latent factor model for high-dimensional and sparse matrices," *IEEE transactions on big data*, vol. 8, no. 3, pp. 784–794, 2020.
- [69] M. Shang, Y. Yuan, X. Luo, and M. Zhou, "An α - β -divergence-generalized recommender for highly accurate predictions of missing user preferences," *IEEE transactions on cybernetics*, vol. 52, no. 8, pp. 8006–8018, 2021.
- [70] D. Cheng, J. Huang, S. Zhang, X. Zhang, and X. Luo, "A novel approximate spectral clustering algorithm with dense cores and density peaks," *IEEE transactions on systems, man, and cybernetics: systems*, vol. 52, no. 4, pp. 2348–2360, 2021.
- [71] W. Qin, X. Luo, and M. Zhou, "Adaptively-accelerated parallel stochastic gradient descent for high-dimensional and incomplete data representation learning," *IEEE Transactions on Big Data*, 2023.
- [72] J. Li, F. Tan, C. He, Z. Wang, H. Song, P. Hu, and X. Luo, "Saliency-aware dual embedded attention network for multivariate time-series forecasting in information technology operations," *IEEE Transactions on Industrial Informatics*, 2023.
- [73] X. Luo, Y. Zhou, Z. Liu, and M. Zhou, "Fast and accurate non-negative latent factor analysis of high-dimensional and sparse matrices in recommender systems," *IEEE Transactions on Knowledge and Data Engineering*, vol. 35, no. 4, pp. 3897–3911, 2021.
- [74] D. Wu, Y. He, and X. Luo, "A graph-incorporated latent factor analysis model for high-dimensional and sparse data," *IEEE Transactions on Emerging Topics in Computing*, 2023.
- [75] W. Yang, S. Li, Z. Li, and X. Luo, "Highly accurate manipulator calibration via extended kalman filter-incorporated residual neural network," *IEEE Transactions on Industrial Informatics*, vol. 19, no. 11, pp. 10831–10841, 2023.
- [76] Z. Li, S. Li, O. O. Bamasag, A. Alhothali, and X. Luo, "Diversified regularization enhanced training for effective manipulator calibration," *IEEE Transactions on Neural Networks and Learning Systems*, vol. 34, no. 11, pp. 8778–8790, 2022.
- [77] F. Ye, Z. Lin, C. Chen, Z. Zheng, and H. Huang, "Outlier-resilient web service qos prediction," in *Proceedings of the Web Conference 2021*, 2021, pp. 3099–3110.
- [78] S. Wang, Y. Ma, B. Cheng, F. Yang, and R. N. Chang, "Multi-dimensional qos prediction for service recommendations," *IEEE Trans. Serv. Comput.*, vol. 12, no. 1, pp. 47–57, 2016.
- [79] X. Su, M. Zhang, Y. Liang, Z. Cai, L. Guo, and Z. Ding, "A tensor-based approach for the qos evaluation in service-oriented environments," *IEEE Trans. Netw. Serv. Manag.*, vol. 18, no. 3, pp. 3843–3857, 2021.
- [80] L. Chen and X. Luo, "Tensor distribution regression based on the 3d conventional neural networks," *IEEE/CAA Journal of Automatica Sinica*, vol. 10, no. 7, pp. 1628–1630, 2023.
- [81] Z. Liu, Y. Yi, and X. Luo, "A high-order proximity-incorporated nonnegative matrix factorization-based community detector," *IEEE Transactions on Emerging Topics in Computational Intelligence*, vol. 7, no. 3, pp. 700–714, 2023.
- [82] W. Li, R. Wang, X. Luo, and M. Zhou, "A second-order symmetric non-negative latent factor model for undirected weighted network representation," *IEEE Transactions on Network Science and Engineering*, vol. 10, no. 2, pp. 606–618, 2022.
- [83] H. Wu, X. Luo, and M. Zhou, "Discovering hidden pattern in large-scale dynamically weighted directed network via latent factorization of tensors," in *2021 IEEE 17th International Conference on Automation Science and Engineering (CASE)*, 2021, pp. 1533–1538.